# Supplementary Table

**Supplementary Table S1 Cryo-ET data collection and reconstruction statistics**

| | Retraction fiber with TSPAN7-GFP | Retraction fiber with engineered TSPAN7 dimer |
|---|---|---|
| Magnification | 64,000 | 64,000 |
| Voltage (kV) | 300 | 300 |
| Pixel size (Å) | 1.36 | 1.36 |
| Camera | Gatan K3 Summit | Gatan K3 Summit |
| Tilt range (°) | +60 to -60 | +60 to -60 |
| Tilt step (°) | 3 | 3 |
| Electron exposure ($e^{-}$/Å$^2$) | 3.2 (per tilt) | 3.2 (per tilt) |
| Defocus range (μm) | -4.5 to -5.5 | -4.5 to -5.5 |
| Raw tomograms | 103 | 114 |
| Subtomograms | 3,675 | 3,572 |
| Reported resolution (Å) | 33 | 16 |
| Symmetry imposed | C6 | C7 |
| EMDB code | EMD-65524 | EMD-65527 |

**Supplementary Table S2 Single-particle cryo-EM data collection and reconstruction statistics**

| | Retraction fiber with engineered TSPAN7 dimer | | |
|---|---|---|---|
| **Data collection** | | | |
| Magnification | 64,000 | | |
| Voltage (kV) | 300 | | |
| Pixel size (Å) | 1.36 | | |
| Camera | Gatan K3 Summit | | |
| Electron exposure ($e^{-}$/Å$^2$) | 50 | | |
| Defocus Range (μm) | -1.2 to -1.8 | | |
| Number of micrographs | 6,171 | | |
| **Reconstruction** | | | |
| | **Spiral** (EMD-65483) | **Tetramer** (EMD-65484; PDB: 9W2D) | **Dimer** (EMD-65485 PDB: 9W2B ) |
| Particles | 105,167 particles | 736,169 particles | 1,472,338 particles |
| Software | CryoSPARC | CryoSPARC | CryoSPARC |
| Reported resolution (Å) (FSC=0.143 threshold) | 7.83 | 6.63 | 5.87 |
| Symmetry imposed | Helical | C2 | C2 |
| **Model statistics** | | | |
| Chains | / | 4 | 2 |
| Atoms | / | 7732 | 3866 |
| Protein residues | / | 1000 | 500 |
| r.m.s. deviations | | | |
| Bonds (Å) | / | 0.002 | 0.002 |
| Angles (°) | / | 0.740 | 0.621 |
| Ramachandran plot | | | |
| Favored (%) | / | 96.77 | 97.58 |
| Allowed (%) | / | 3.23 | 2.42 |
| Outliers (%) | / | 0.00 | 0.00 |
| MolProbity score | / | 1.85 | 1.66 |
| Clash score | / | 13.91 | 11.39 |
| Rotamer outliers (%) | / | 0.00 | 0.00 |

## Supplementary figures

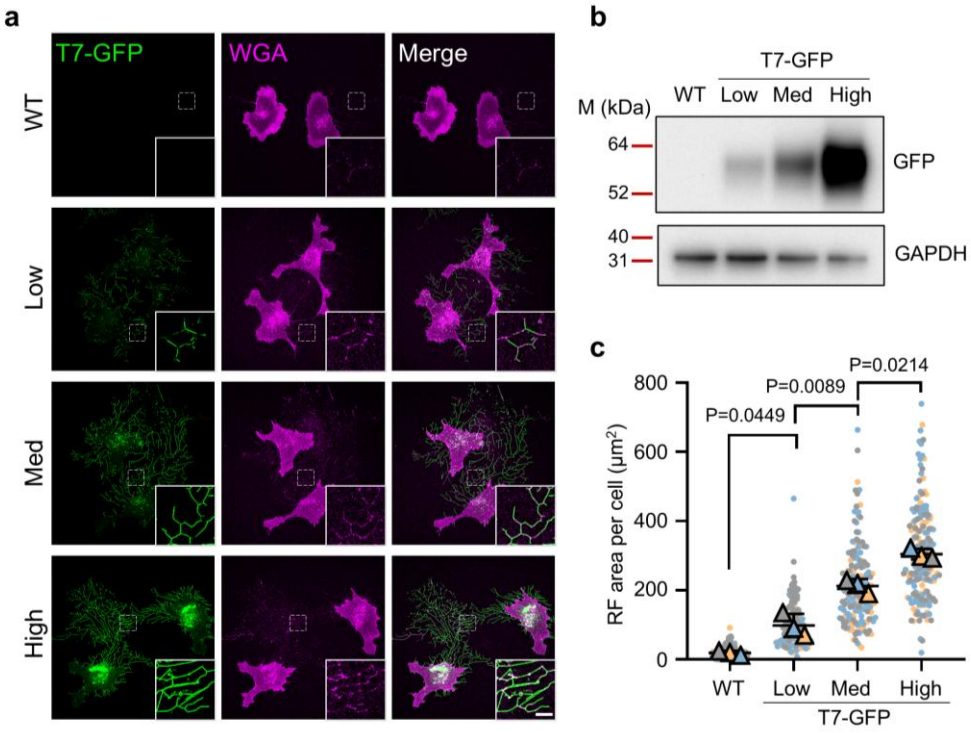


**Supplementary Fig. S1 TSPAN7 promotes the formation of retraction fibers in a dose-dependent manner.**

**a** Representative confocal images of wild-type NRK cells or NRK cells stably expressing different levels of TSPAN7-GFP (Low, Med, and High). Cells were stained with WGA-TMR.

**b** Western-blot analysis showing the expression levels of TSPAN7-GFP in the 3 different cell lines from **a**.

**c** Statistical analysis of the area of retraction fibers per cell in **a**. *n* = 169, 165, 168 and 180 cells were analyzed for WT, T7-Low, T7-Med, and T7-High, respectively.

Scale bars, 5 μm.

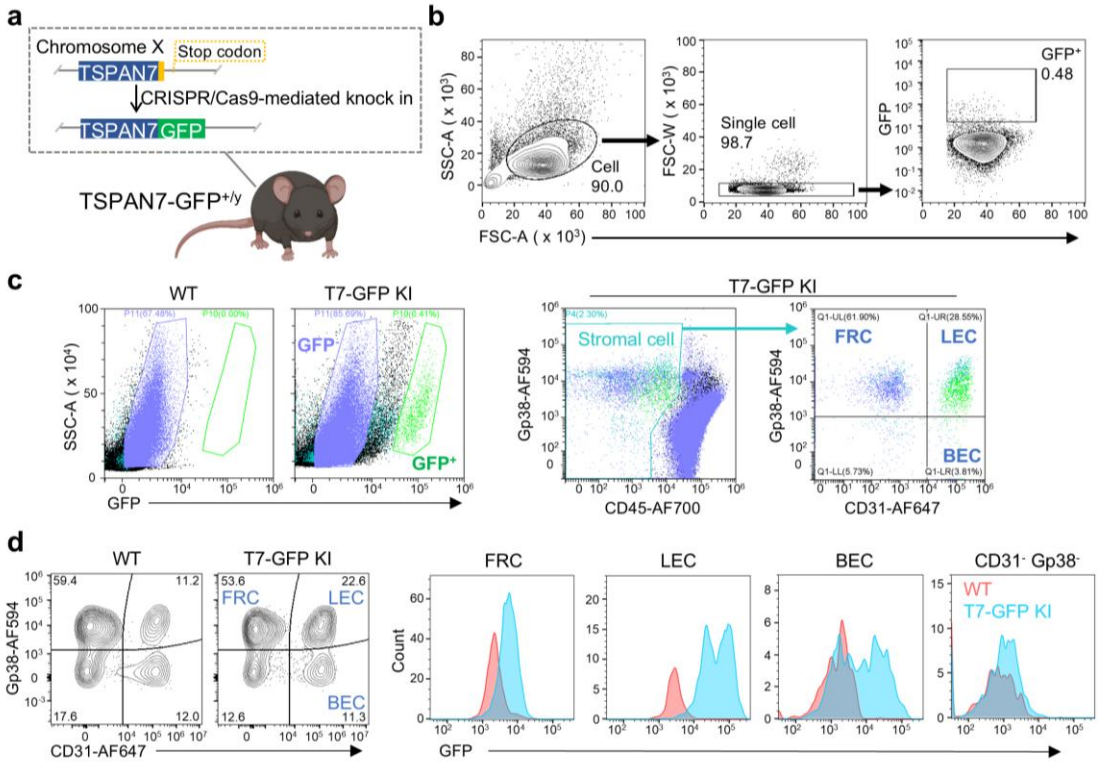


**Supplementary Fig. S2 Identification of GFP$^+$ cells in mouse lymph nodes.**

**a** Schematic illustration of the construction of the TSPAN7-GFP knock-in (T7-GFP KI) mouse strain. The stop codon of TSPAN7 was replaced with the coding sequence of GFP using the CRISPR/Cas9 system.

**b** The flow cytometry gating strategy that was used in isolating GFP$^+$ cells from mouse lymph nodes.

**c** Representative flow cytometry plots of GFP$^+$ cells in lymph nodes from WT and TSPAN7-GFP knock-in mice (left) and the gating strategy for analyzing GFP$^+$ lymph node stromal cell populations (right) including FRCs (fibroblastic reticular cells), LECs (lymphatic endothelial cells), and BECs (blood endothelial cells).

**d** Representative flow cytometry plots (left panel) of lymph node stromal cell populations and mean fluorescence intensity (MFI) of GFP (right panel) in different populations from WT and T7-GFP KI mice.

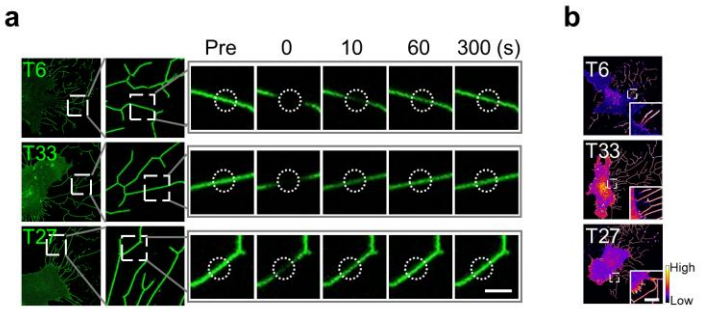


**Supplementary Fig. S3 Analysis of TSPAN6, TSPAN27 and TSPAN33 on retraction fibers, related to Fig. 2.**

**a** Related to Fig. 2i. Representative time-lapse images of FRAP assays on the retraction fibers of NRK cells expressing TSPAN6-GFP (T6), TSPAN27-GFP (T27) or TSPAN33-GFP (T33). The right panels show enlarged areas from the left panels. The dashed circles represent areas of bleaching.
**b** Related to Fig. 2j. The fluorescence intensities of TSPAN6-GFP (T6), TSPAN27-GFP (T27) and TSPAN33-GFP (T33) are shown as heatmaps.
Scale bars, 2 μm in **a**; 5 μm in **b**.

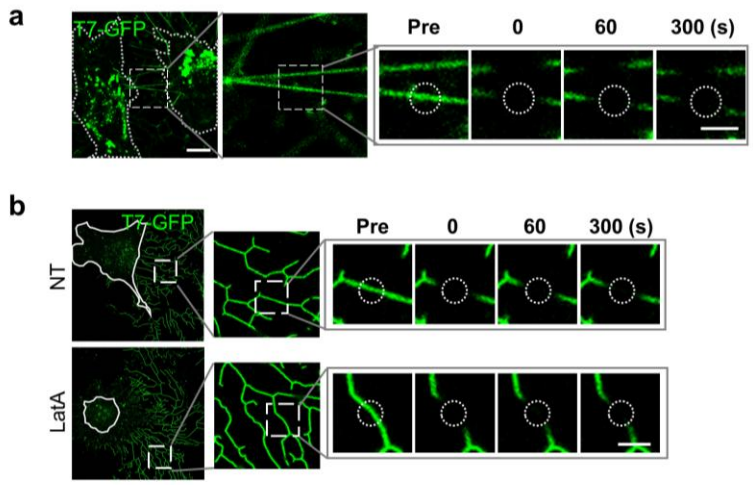


**Supplementary Fig. S4 TSPAN7 is immobile on TNTs, related to Fig. 2.**

**a** Related to Fig. 2k. Representative time-lapse images of FRAP assays on the TNTs of T7-GFP-expressing NRK cells. Cell contours are highlighted with dashed white lines. The right panels show enlarged areas from the left panels. The dashed circles represent areas of bleaching.

**b** Related to Fig. 2l. Confocal images of cells pretreated with 2 μM latrunculin A (LatA) or control solvent (ethanol, NT) before FRAP assay are shown in the left panel. Cell contours are highlighted with white lines. The right panels show enlarged areas from the left panels. The dashed circles represent areas of bleaching.

Scale bars, 10 μm in **a** (left panel); 2 μm in enlarged areas in **a** and **b**.

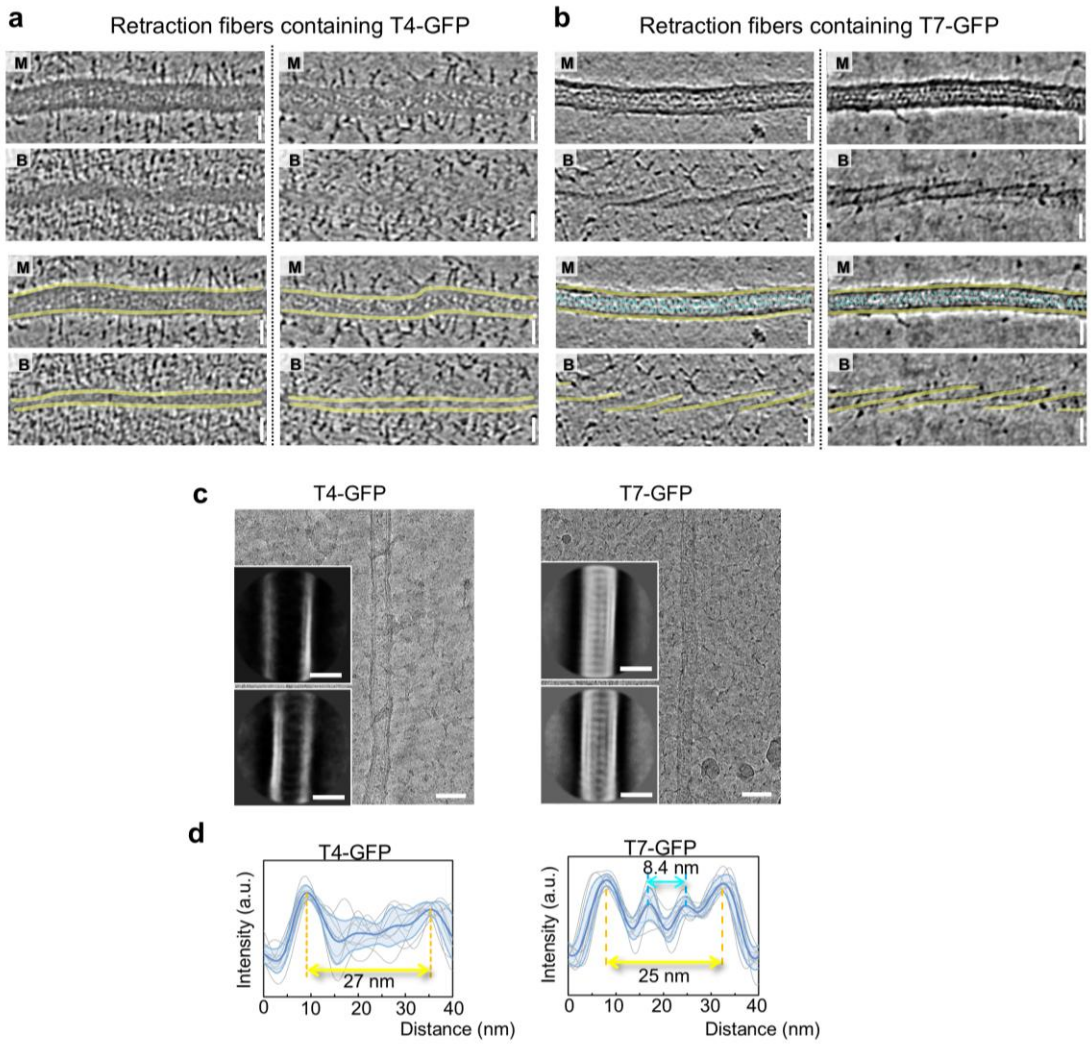


**Supplementary Fig. S5 Representative cryo-ET reconstructions of TSPAN4-GFP and TSPAN7-GFP retraction fibers.**

**a** The middle (M) and bottom (B) slices of two additional TSPAN4-GFP retraction fiber tomograms are shown. The retraction fiber boundaries in different slices are labeled with yellow lines.
**b** The middle (M) and bottom (B) slices of two additional TSPAN7-GFP retraction fiber tomograms are shown. The yellow lines outline the retraction fiber boundaries in different slices, and the cyan markers indicate the density of the regular dots (GFP) on the cytoplasmic side of the cell membrane.
**c** Two-dimensional classification results of particles picked from the single-particle cryo-EM micrographs of *in situ* retraction fibers with TSPAN4-GFP (left) or TSPAN7-GFP (right).
**d** Intensity profiles of lines ($n$ = 9) across the middle slices of tomograms of retraction fibers containing TSPAN4-GFP (left) or TSPAN7-GFP (right) are plotted and aligned together. The deep blue lines are the averaged traces for all plots. The light blue lines are the averaged traces with the standard deviation. Distances separating intensity peaks are indicated for retraction fiber boundary densities (yellow double-headed arrow) and luminal protein densities (blue double-headed arrow). a.u., arbitrary units.
Scale bars, 30 nm.

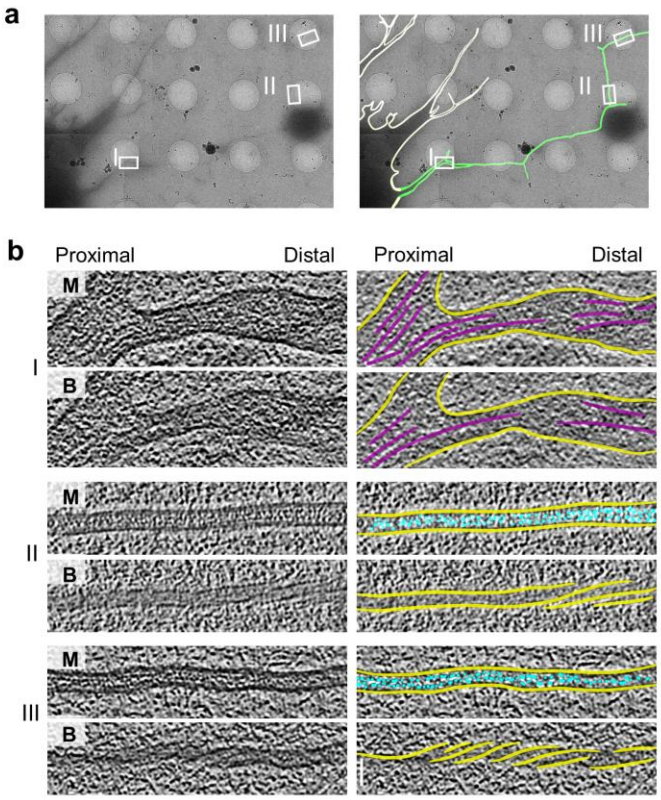


**Supplementary Fig. S6 Cryo-ET characterization of the spiral assembly of TSPAN7 on retraction fibers attached to cells.**

**a** Left: Representative low-magnification cryo-EM micrograph showing retraction fibers extending from the cell body. Right: The same image with the cell boundary indicated by white lines and retraction fibers indicated by green lines.

**b** Left: Middle (M) and bottom (B) slices of the tomograms corresponding to the three areas labeled as I-III in **a**. Right: The same images with F-actin labeled in magenta, the cell membrane in yellow, and GFP in cyan.

Scale bar, 30 nm.

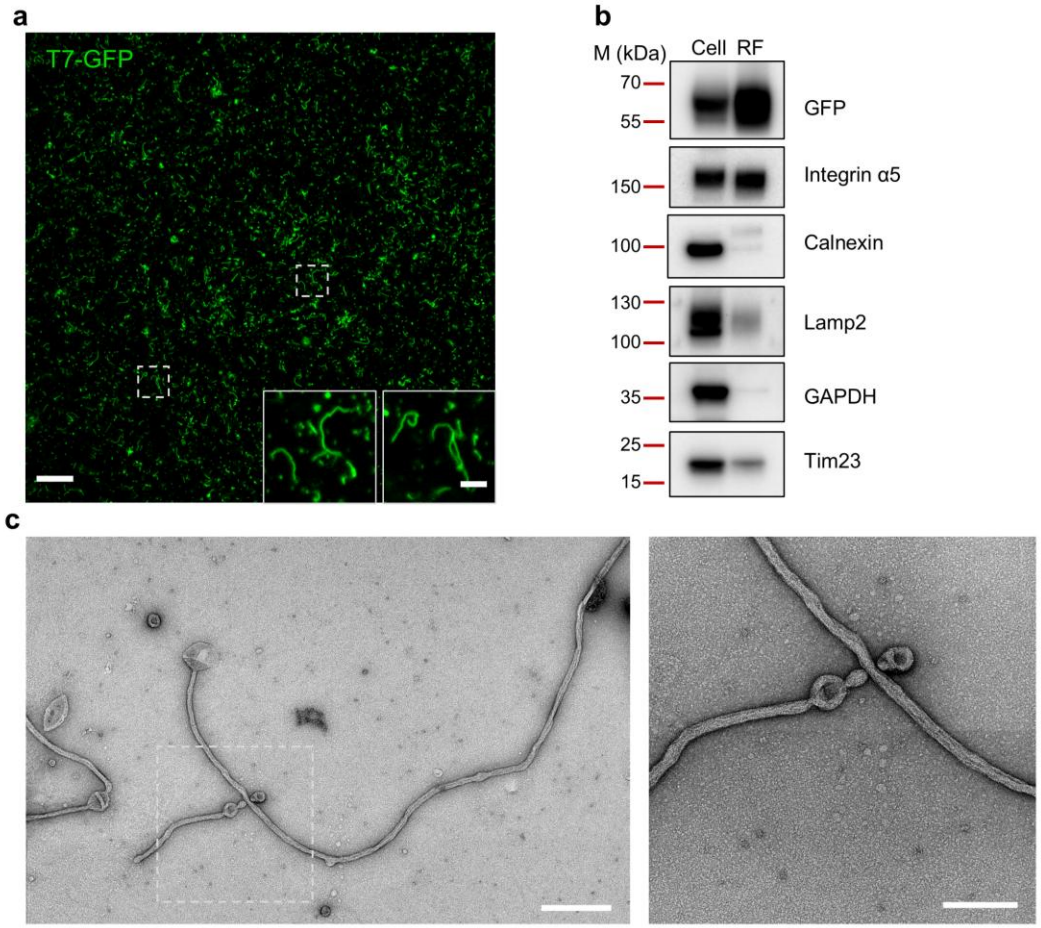


**Supplementary Fig. S7 Characterization of isolated retraction fibers.**

**a** Representative confocal image of retraction fibers isolated from NRK cells stably expressing TSPAN7-GFP.

**b** Western-blot analysis of cell bodies (Cell) or retraction fibers (RF). Equal amounts of protein were loaded for the two samples.

**c** Representative negative-stain EM images of isolated retraction fibers from NRK cells stably expressing TSPAN7-GFP. The right panel shows a magnified view of the region indicated by the white dashed box in the left panel.

Scale bars, 10 μm in **a**; 2 μm in inserts in **a**; 500 nm in the left panel in **c**; 200 nm in the right panel in **c**.

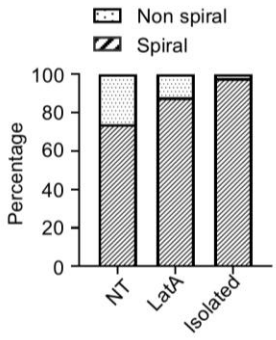


**Supplementary Fig. S8 The effect of different treatment conditions on TSPAN7 spiral formation on retraction fibers.**

Cryo-EM tilt series were collected from 76 retraction fibers (RFs) from untreated cells (NT), 75 RFs from LatA-treated cells, and 45 isolated RFs. Following tomogram reconstruction, each fiber was classified as either “Non-spiral” or “Spiral”. Quantitative analysis revealed spiral configurations in 74% (NT), 88% (LatA-treated), and 98% (isolated) of cases.

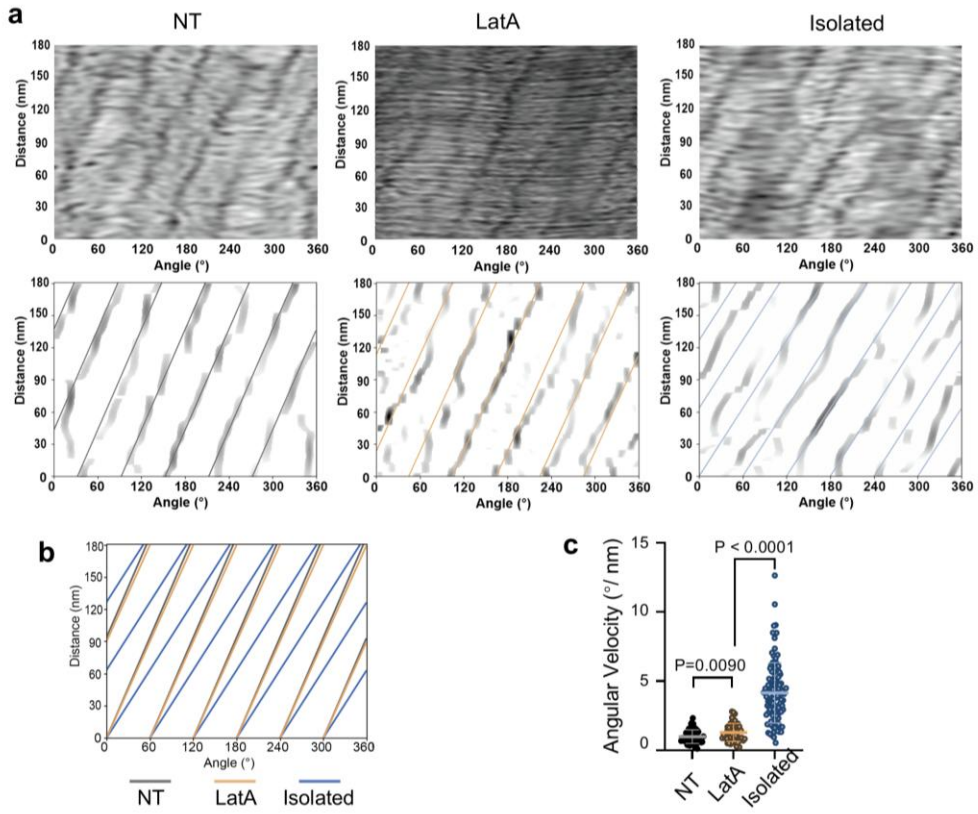


**Supplementary Fig. S9 The effect of different treatment conditions on the protofilament winding parameters in TSPAN7 spirals.**

**a** Helical unfolding analysis of representative tomograms of retraction fibers (RFs) from untreated cells (NT), RFs from LatA-treated cells, and isolated RFs. Top: Original unfolded tomograms. Bottom: Corresponding filtered and feature-extracted images, as well as the fitted helical crest.
**b** Superimposed spiral crest fittings from panel **a**.
**c** Plotting of the angular velocity of the TSPAN7 spirals to assess their tightness. *n*=52 randomly selected spiral structures from each of the three groups were analyzed. Data were plotted as mean ± SD.

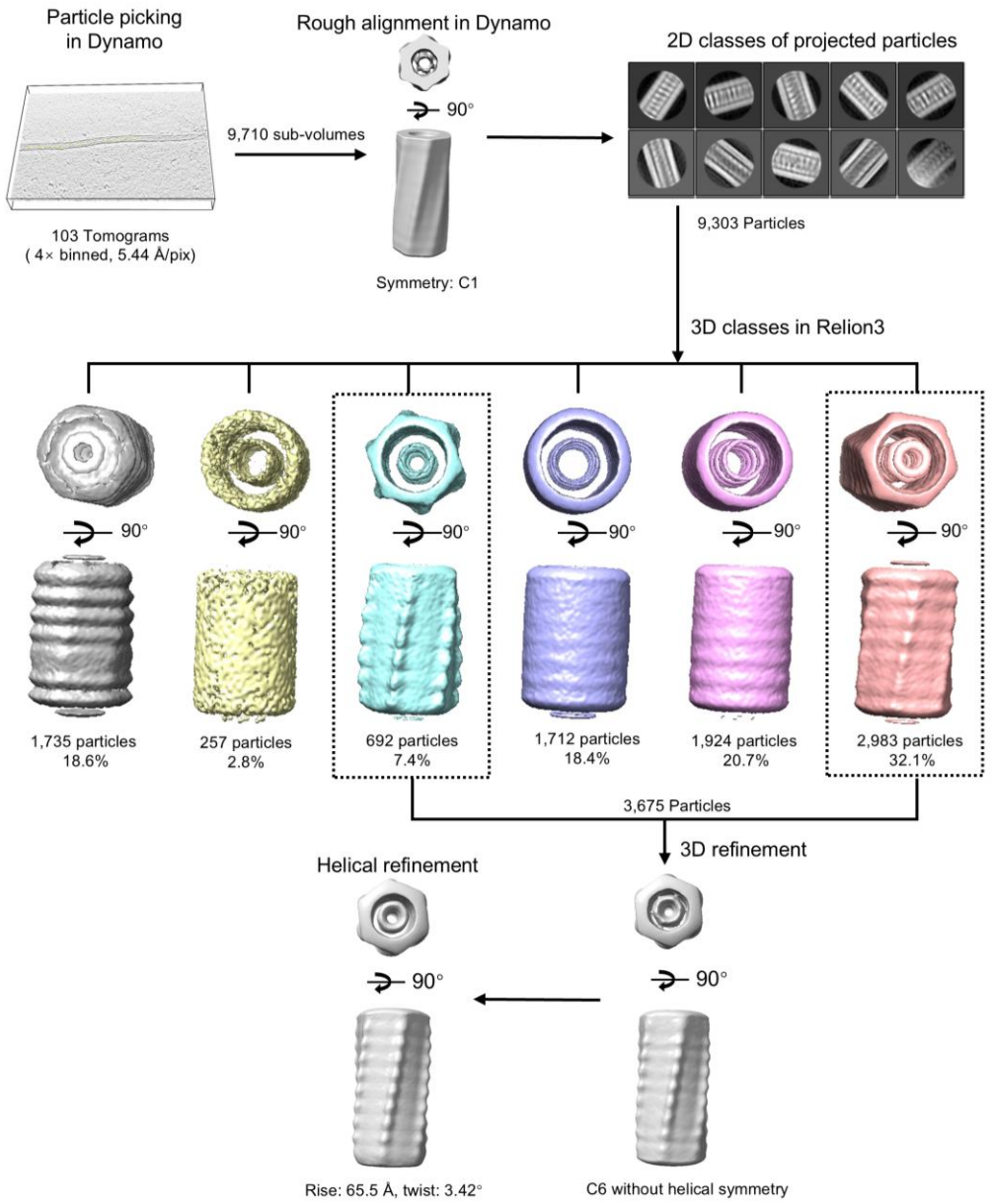


**Supplementary Fig. S10 Workflow of subtomogram averaging analysis for isolated TSPAN7-GFP retraction fibers.**

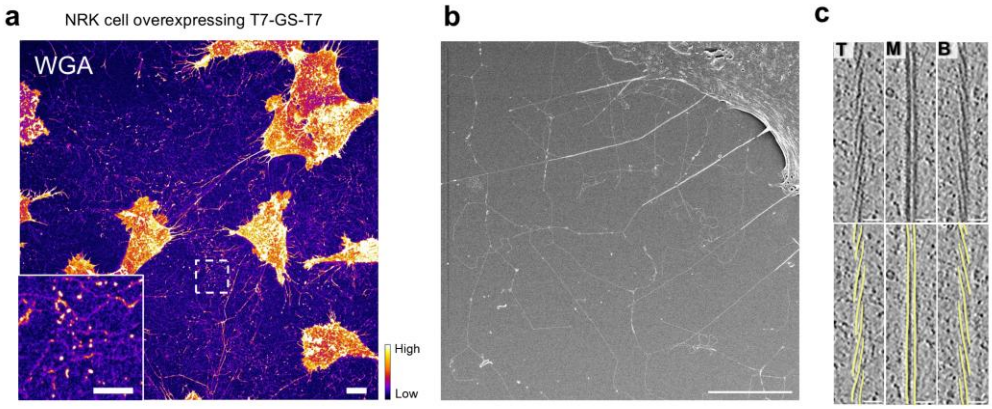


**Supplementary Fig. S11 Characterization of *in situ* retraction fibers containing the engineered TSPAN7 dimer.**

**a** Representative confocal image of NRK cells stably expressing the engineered TSPAN7 dimer and stained with WGA-TMR. The intensity of the fluorescent signal is shown as a heatmap.
**b** Representative SEM image of an NRK cell stably expressing the engineered TSPAN7 dimer.
**c** Representative tomogram slices of the *in situ* retraction fibers containing engineered TSPAN7 dimers. See also Supplementary Video S8.
Scale bars, 10 µm in **a**; 5 µm in **b**; 30 nm in **c**.

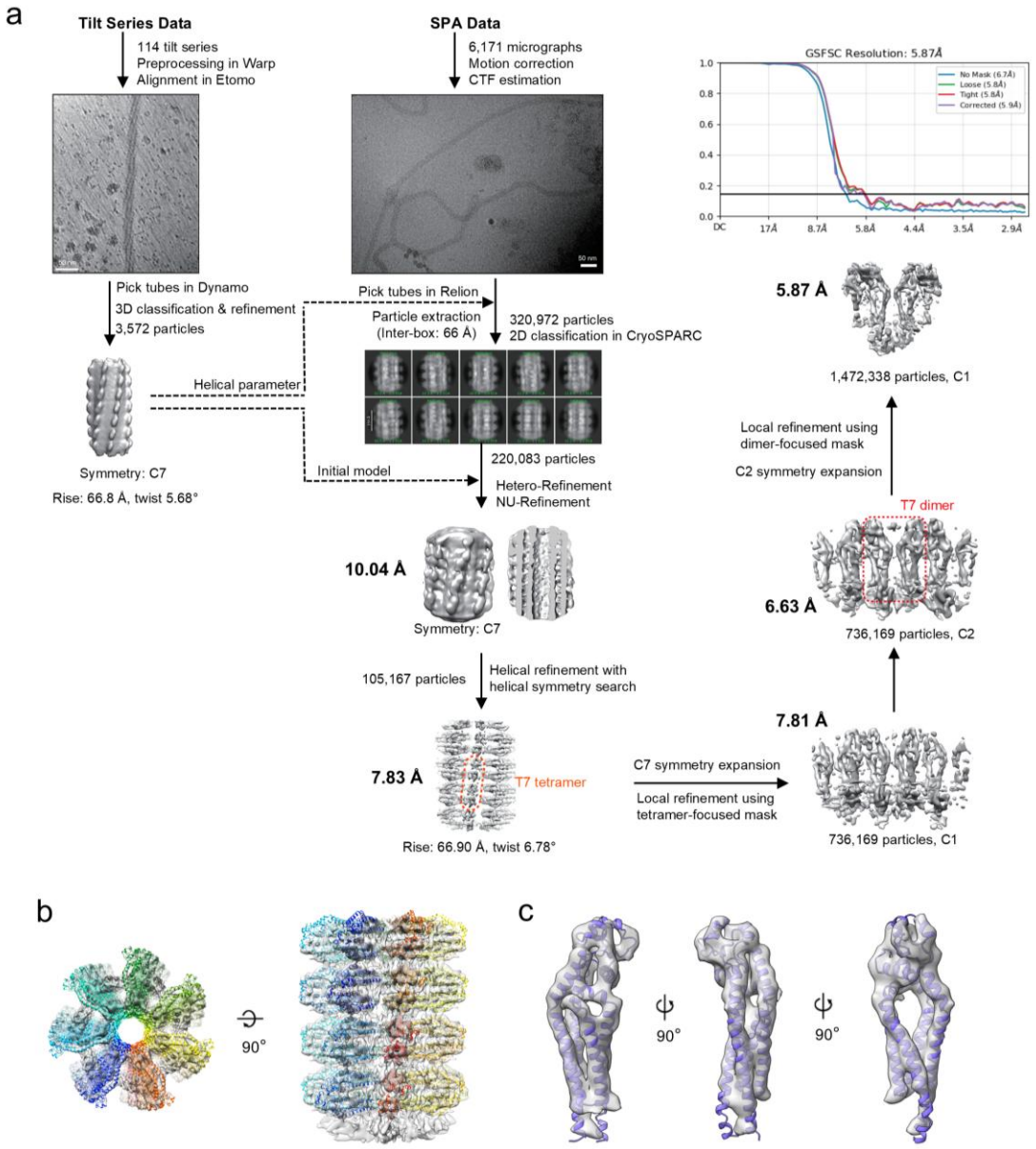


**Supplementary Fig. S12 Cryo-EM reconstruction of retraction fibers containing engineered TSPAN7 dimers.**

**a** Workflow of cryo-EM data processing.

**b** TSPAN7 spiral density map with fitted atomic model.

**c** TSPAN7 monomer density extracted from the spiral map with fitted atomic model.

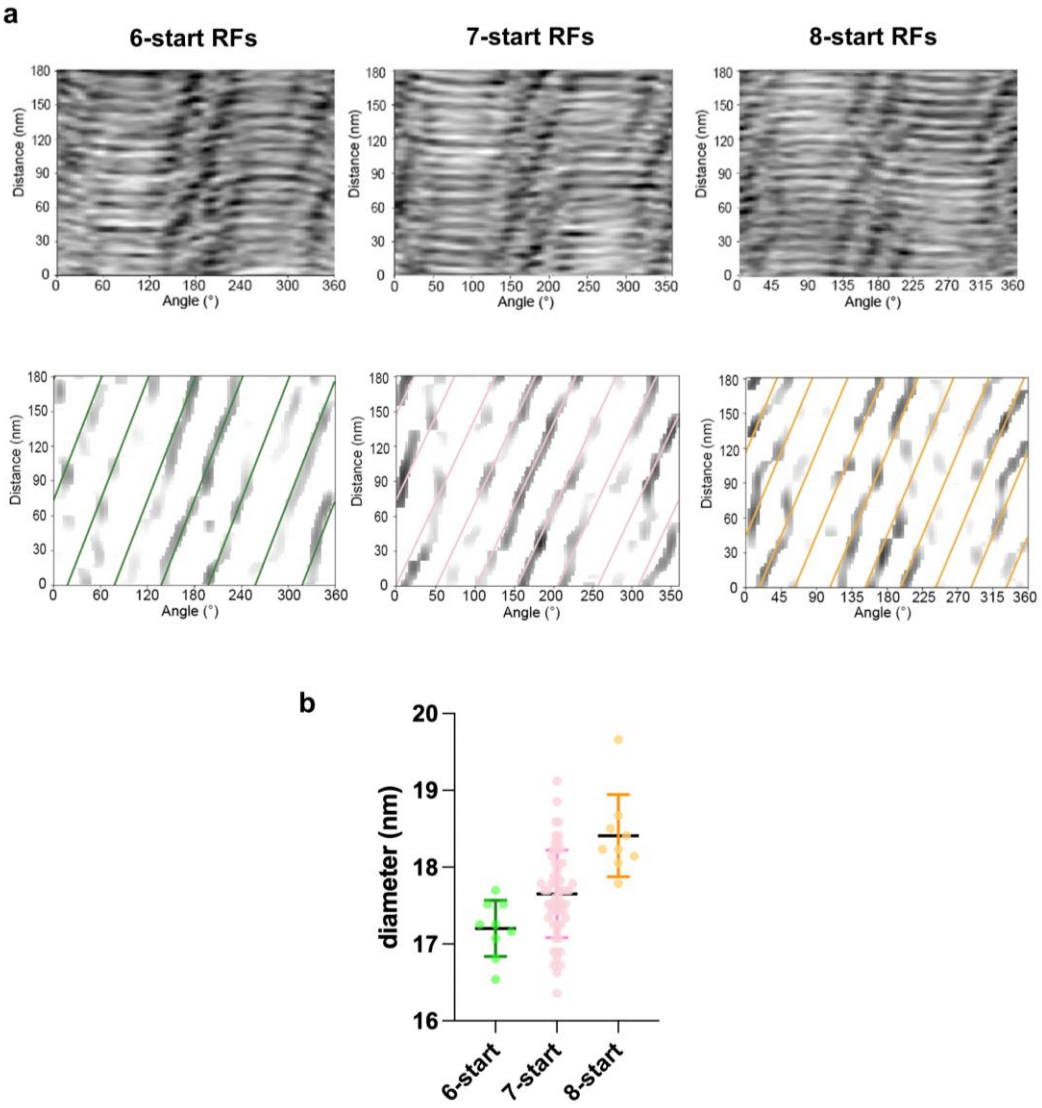


**Supplementary Fig. S13 Heterogeneity analysis of retraction fibers (RFs) containing engineered TSPAN7 dimers.**

**a** Helical unfolding analysis of representative tomograms from retraction fibers (RFs) containing engineered TSPAN7 dimers.

**b** From our collected datasets, we identified TSPAN7 spirals with 6-start ($n$ = 9), 7-start ($n$ = 57), and 8-start ($n$ = 9) configurations. Their diameters were measured and plotted as mean ± SD: 6-start TSPAN7-GFP RFs have an averaged diameter of 17.20 ± 0.31nm, 7-start RFs have an averaged diameter of 17.69 ± 0.53 nm, and 8-start RFs have an averaged diameter of 18.35 ± 0.35 nm.

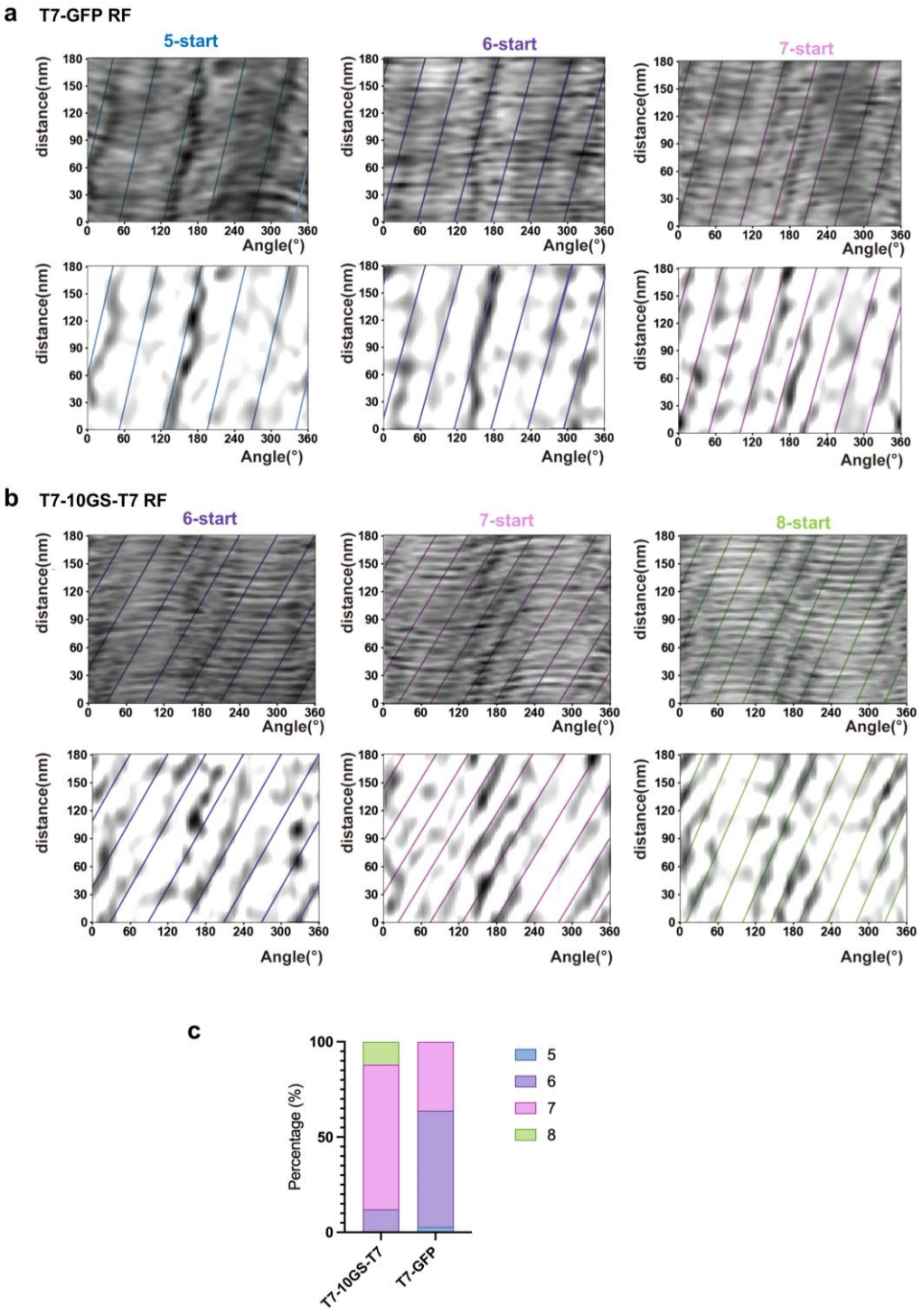


**Supplementary Fig. S14 Helical unfolding and statistical analysis of representative tomograms of retraction fibers (RFs) containing TSPAN7-GFP (T7-GFP) or engineered TSPAN7 dimers (T7-10GS-T7).**

**a, b** Representative helical unfolding analysis of tomograms of RFs containing T7-GFP (**a**) or engineered T7-10GS-T7 (**b**). We observed 5-, 6-, and 7-start helical configurations for T7-GFP spirals, whereas 6-, 7-, and 8-start configurations for engineered TSPAN7 dimer spirals.

**c** Quantification of helical start distributions. For T7-GFP spirals ($n$ = 108): 3% (5-start), 61% (6-start), and 36% (7-start). For the dimer T7-10GS-T7 spirals ($n$ = 75): 12% (6-start), 76% (7-start), and 12% (8-start).

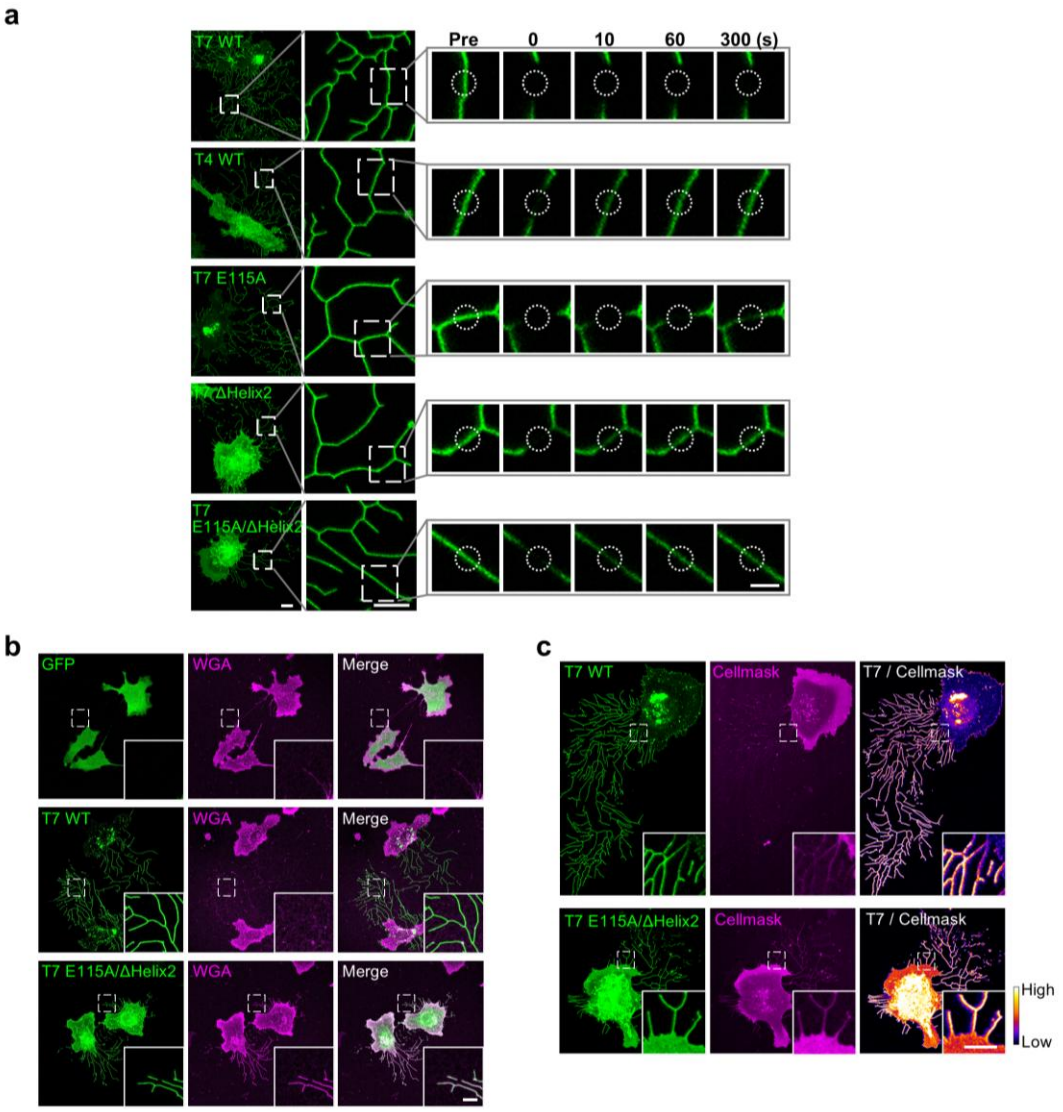


**Supplementary Fig. S15 Subcellular distribution and molecular dynamics of TSPAN7 mutants in NRK cells.**

**a** Related to Fig. 5e. Representative time-lapse images of FRAP assays performed on the retraction fibers of NRK cells expressing wild-type TSPAN7-GFP (T7 WT), wild-type TSPAN4-GFP (T4 WT), single-site mutants of TSPAN7-GFP (T7 E115A or T7 ΔHelix2) and the double mutant of TSPAN7-GFP (T7 E115A/ΔHelix2). The right panels show enlarged areas from the left panels. The dashed circles represent areas of bleaching.

**b** Related to Fig. 5f. Representative confocal images of NRK cells expressing GFP, wild-type TSPAN7-GFP (T7 WT) or double mutant TSPAN7-GFP (T7 E115A/ΔHelix2) and stained with WGA-TMR (WGA).

**c** Related to Fig. 5g. Representative confocal images of NRK cells expressing wild-type TSPAN7-GFP (T7 WT) or double mutant TSPAN7-GFP (T7 E115A/ΔHelix2). The fluorescence intensities of T7 WT and T7 E115A/ΔHelix2 are shown as heatmaps.

Scale bars, 5 μm in **a** (left), **b** and **c**; 2 μm in **a** (right).

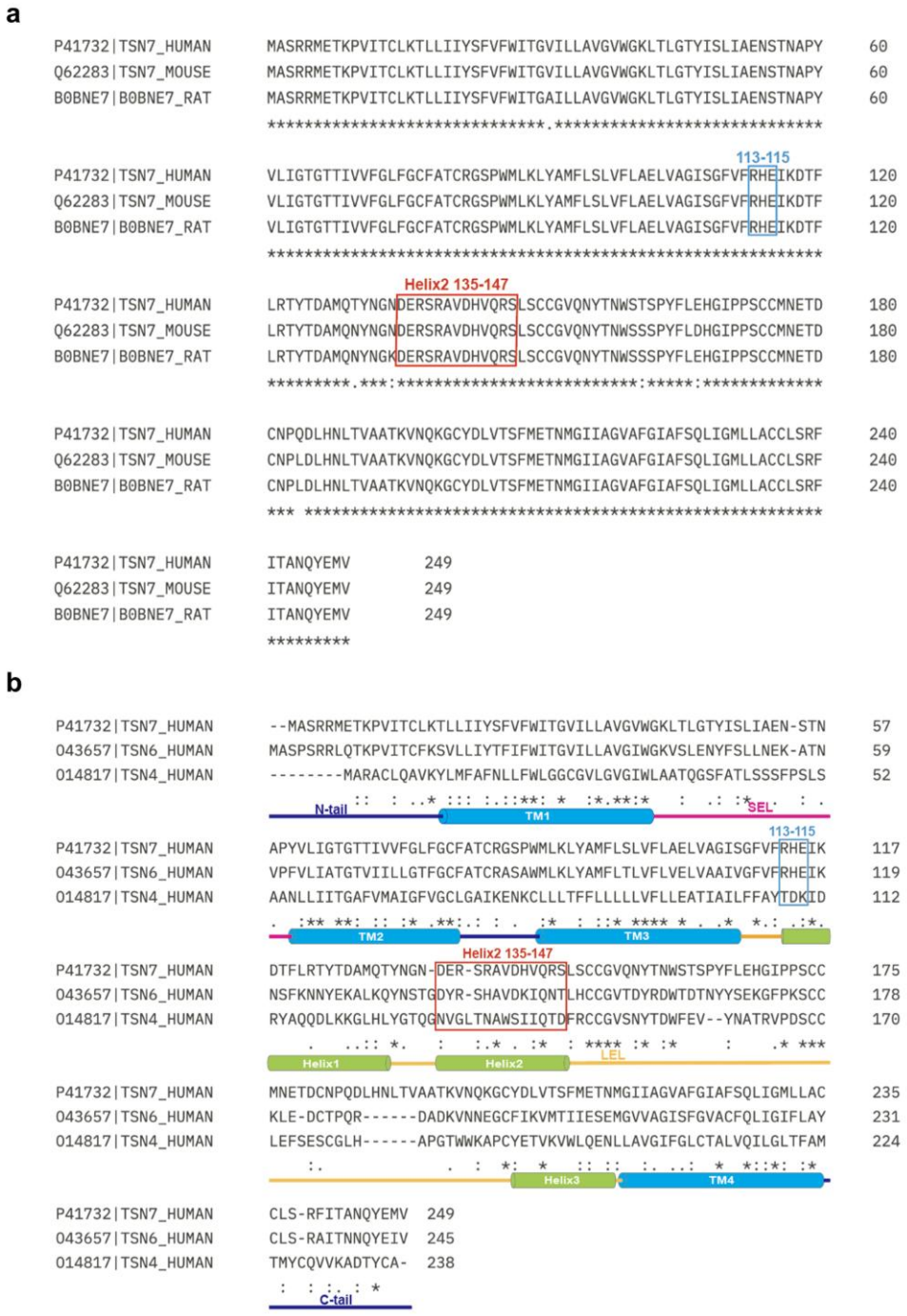


**Supplementary Fig. S16 Tetraspanin sequence alignment.**

**a** Sequence alignment of TSPAN7 from *H. sapiens*, *M. musculus*, and *R. norvegicus*, conducted with Cluster Omega. Colored boxes mark the two oligomer interaction sites, E115 and Helix 2 (aa 135–147).

**b** Sequence alignment of human TSPAN7, TSPAN6, and TSPAN4 proteins, conducted with Cluster Omega. Topological domains are indicated below the sequences. Colored boxes mark the two TSPAN7 oligomer interaction sites, E115 and Helix 2 (aa 135–147).

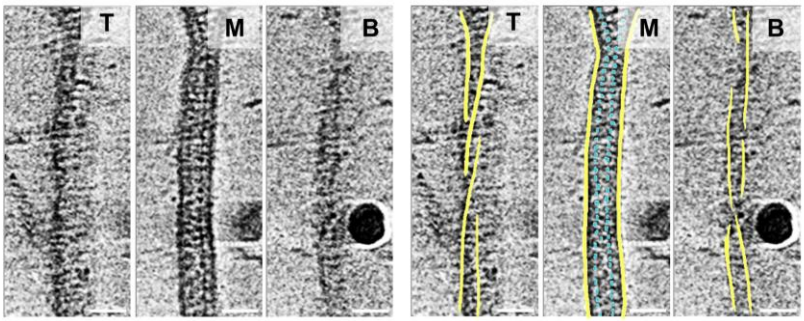


**Supplementary Fig. S17 Cryo-ET characterization of retraction fibers with TSPAN6-GFP.**

Representative bottom (B), middle (M), and top (T) slices of the reconstructed tomogram of the retraction fiber. Yellow lines outline the boundaries of the membrane tube in different slices, and cyan markers indicate densities of regularly spaced dots (GFP tags) on the cytoplasmic side of the membrane. See also Supplementary Video S10. Scale bars, 30 nm.

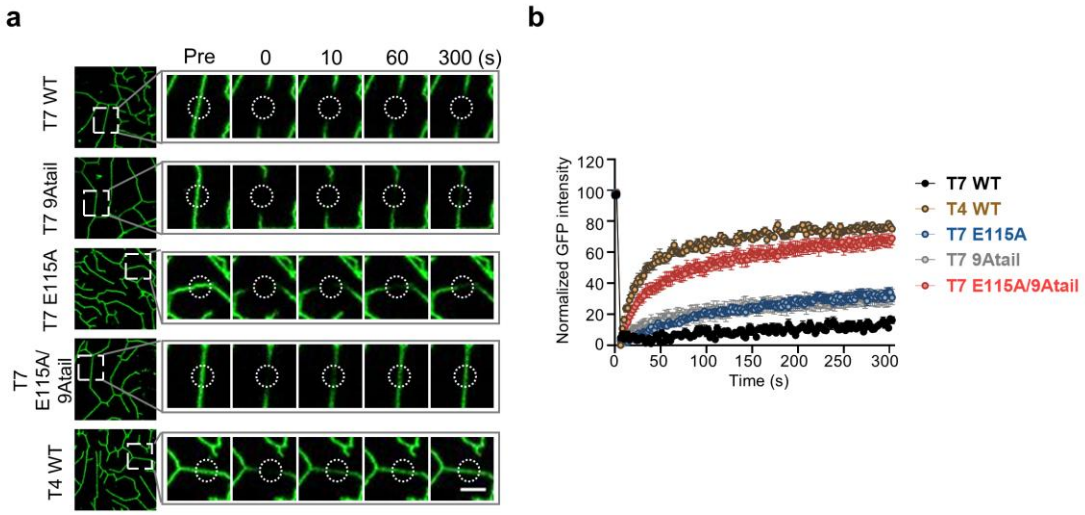


**Supplementary Fig. S18 Role of the TSPAN7 intracellular region in its polymerization.**

**a** Representative time-lapse images of FRAP assays on the retraction fibers of NRK cells expressing wild-type TSPAN7-GFP (T7 WT), TSPAN7 single mutant (T7 E115A or T7 9Atail), TSPAN7 double mutant (T7 E115A/9Atail) or wild-type TSPAN4-GFP (T4 WT). The right panels show enlarged areas from the left panels. The dashed circles represent areas of bleaching.
**b** The fluorescence intensities in bleached areas in **a** were tracked and plotted. For each curve, data from 9 (for T7 WT, T7 E115A and T7 9Atail), 15 (for T7 E115A/9Atail) or 8 (for T4 WT) bleached areas were normalized and plotted as mean ± SEM.
Scale bar, 2 μm,

## Supplementary video titles

**Supplementary Video S1. Time-lapse imaging of the spreading process of a protein-free GUV in the *in vitro* reconstitution assay.**

**Supplementary Video S2. Time-lapse imaging of the spreading process of a TSPAN7-GFP-embedded GUV in the *in vitro* reconstitution assay.**

**Supplementary Video S3. Time-lapse imaging of a migrating NRK cell expressing TSPAN7-GFP and stained with SiR-actin.**

**Supplementary Video S4. Tomogram of a retraction fiber containing TSPAN7-GFP.**

**Supplementary Video S5. Tomogram of a retraction fiber containing TSPAN4-GFP.**

**Supplementary Video S6. Tomogram of a retraction fiber containing TSPAN7-HA.**

**Supplementary Video S7. Tomogram of a retraction fiber of LEC isolated from TSPAN7-GFP knock-in mouse.**

**Supplementary Video S8. Tomogram of a retraction fiber containing engineered TSPAN7 dimer.**

**Supplementary Video S9. Tomogram of a retraction fiber containing TSPAN7 E115A/ΔHelix2-GFP.**

**Supplementary Video S10. Tomogram of a retraction fiber containing TSPAN6-GFP.**

**Supplementary Video S11. Time-lapse imaging showing the formation of tubular membranes in NRK cells under shear stress. Cells are stably expressing TSPAN7-GFP (left) or TSPAN7 E115A/ΔHelix2-GFP (right).**